Internodal myelination during development quantitated using X-ray diffraction

Deepika Agrawal, Rachel Hawk, Robin L. Avila, Hideyo Inouye, Daniel A. Kirschner *

Biology Department, Boston College, 140 Commonwealth Ave (Higgins Hall), Chestnut Hill, MA 02467-3811, USA

ABSTRACT

Characterizing the formation, accretion, and stability of myelin during development, maturation, and senescence is important for better understanding critical periods in the function of the nervous system in normal growth and following environmental insult or genetic mutation. Although there are numerous studies on the ultrastructural, biochemical, and genetic aspects of myelin development and maturation, few have used X-ray diffraction (XRD), which can rapidly provide unique metrics about internodal myelin based on measurements from whole, unfixed tissue. Besides periodicity (the classic attribute of internodal myelin measured by XRD), other parameters include: relative amount of myelin, membrane dimensions, and packing disorder. To provide a baseline for future experiments on myelin structural integrity, we used XRD to characterize internodal myelin as a function of age (from 5 to 495 days) in the mouse, a species increasingly used for developing transgenic models of human neurological diseases. As expected, the relative amount of myelin increased with age in both PNS and CNS, with the most rapid accumulation occurring in the youngest age group. Changes in rate of myelin accretion yielded three distinct age brackets during which small but significant changes in structural parameters were detected: in PNS, myelin period increased, packing distortion decreased, width of extracellular apposition (EXT) decreased, and widths of cytoplasmic apposition (CYT) and lipid bilayer (LPG) increased; in CNS, myelin period decreased, packing distortion decreased, EXT and CYT decreased, and LPG increased. We propose that the data obtained here can serve as a basis for rapidly detecting abnormal pathologies during myelination.

1. Introduction

Nerve conduction in vertebrates is greatly speeded up by the ensheathment of its axons with myelin, an insulating, multilamellar membrane assembly (Lazzarini, 2004). Internodal myelin, which is the portion of the sheath between nodes of Ranvier, consists of membrane pairs that are closely apposed, adhering at their cytoplasmic and extracellular appositions. Compared to other membranes that are loci for enzymatic activities, internodal myelin has a high lipid-to-protein ratio (Norton and Poduslo, 1973). The proteins in compact myelin include P0, MBP, PMP-22, and P2 in PNS, and PLP and MBP in the CNS (Kursula, 2008; Simons and Trotter, 2007; Trapp and Kidd, 2004). The recent co-localization of MBP and ATP synthase in optic nerve myelin (Ravera et al., 2009) may indicate a more active physiological role for compact myelin. The protein composition is the predominant determinant of myelin's periodicity, as the thickness of the membrane bilayer is fairly constant across species whereas the extent of close apposition between bilayers—or membrane packing—varies considerably (Kirschner and Blaurock, 1992; Kirschner et al., 1989). Depending

on animal species the periodicity ranges from 160 to 185 Å in the PNS, and 150 to 170 Å in the CNS.

Both ultrastructural and biochemical approaches have been used to follow myelination. For example, electron microscopy reveals that for PNS myelin the ratio of the number of myelin layers to the axon area rapidly increases during the first 75 days (Friede and Samorajski, 1967; Low, 1976). Based on biochemical metrics of brain weight, myelin yield, and accumulation of MBP and specific myelin lipids, CNS myelination shows an initial rapid increase followed by a more gradual increase (Barbarese et al., 1978; Morell et al., 1972; Norton and Poduslo, 1973; Uzman and Rumley, 1958). The few XRD studies that have been undertaken to characterize myelin accretion and changes in myelin structure with age show that within the first few weeks there is an initial rapid accumulation of PNS and CNS myelin and small changes in their periods (Kirschner and Sidman, 1976; Mateu et al., 1990, 1991; Vargas et al., 2000).

To quantitate more thoroughly the formation and development of internodal myelin and its growth trends, we used XRD with an electronic detector to analyze whole nerves in both the PNS and CNS as a function of age. The advantage of this technique is the rapidity of the measurements, the large sampling volume due to the use of intact nerves, and the fact that the tissue is unfixed

---

* Corresponding author. Fax: +1 617 552 2011.
E-mail address: kirschnd@bc.edu (D.A. Kirschner).

(Avila et al., 2005). We found that the most rapid rate of myelin accretion occurred during the first 3–4 weeks in the PNS and the first 5 weeks in the CNS, and this was followed by a dramatic and progressive decrease in rate. In parallel, the myelin period increased in the PNS and decreased in the CNS. The mean distortion in period decreased with age, suggesting greater structural stability in membrane packing. Underlying the periodicity changes, the membrane bilayer structure showed small changes: whereas the lipid bilayer width increased with age and the width of the extracellular apposition decreased in both PNS and CNS myelins, the cytoplasmic apposition width increased in the PNS but decreased in the CNS. The detailed characteristics quantified here may serve as a benchmark for understanding the dynamic interactions that occur in this multilamellar membrane assembly in diseases where genetic or acquired abnormalities underlie a defect in the myelination program.

2. Materials and methods

The ages of the mice (DDY strain; originally obtained from Clea Japan, Inc.) ranged from 5 to 495 days. Mice were sacrificed by cervical dislocation. Optic and sciatic nerves were maintained moist with Ringers solution during dissection, tied off using surgical silk, and immediately placed in physiological saline (pH 7.4). The nerves, devoid of adhering blood vessels, etc., were inserted into quartz capillaries (0.7 mm for sciatic nerves and 0.5 mm for optic nerves) which were filled with saline and sealed at both ends with dental wax and nail-polish. The procedures for animal use adhered to the NIH Guide for the Care and Use of Laboratory Animals, to which Boston College adheres.

X-ray diffraction experiments and analysis were conducted using our standard lab protocols (Avila et al., 2005). X-ray diffraction patterns, each of 1 hour duration, were recorded using a linear, position-sensitive detector (Molecular Metrology, Inc., Northampton, MA), and analyzed using PeakFit (Jandel Scientific, San Rafael, CA). The positions of the intensity maxima in the diffraction patterns were used to calculate the myelin period. Background intensity (B), approximated as a polynomial curve, was subtracted from the total intensity ($M + B$), and the total integral area of the Bragg peaks coming from the myelin (M), was obtained. We define the relative amount of myelin by the quotient ($\frac{M}{M+B}$), where the total intensity coming from the multilamellar myelin (M, or the peak intensities above background) is divided by the total intensity coming from the volume of nerve subtended by the X-ray beam (or $M + B$), as previously described (Avila et al., 2005). Membrane packing irregularity (Δ), also termed lattice or stacking disorder, results from the statistical displacement of the myelin membranes from the equilibrium positions defined by a perfect myelin lattice. This displacement, which originates from thermal vibrations and from the fluctuating molecular contacts between membrane faces, was determined by analyzing the peak-widths in the diffraction patterns (Alexander, 1979; Avila et al., 2005; Inouye et al., 1989). The percent distortion in period is $\frac{\Delta}{d} \times 100\%$, where d is the myelin period. The intensities $I(h)$ of the individual Bragg peaks were used to calculate the structure amplitudes according to $|F(h)| = \sqrt{hI_{obs}(h)}$. The structure factors $F(h)$ were used to calculate membrane profiles $\rho(r)$ according to $\rho(r) = F(0)/d + (2/d)\sum_{h=1}^{h_{max}} \pm F(h/d)\cos(2\pi rh/d)$, with the phases ($\pm$) determined as described (Caspar and Kirschner, 1971; Kirschner and Ganser, 1982; Kirschner et al., 1989). The electron density profiles provided measures of the widths EXT and CYT of the intermembrane spaces at the extracellular and cytoplasmic appositions, respectively, as well as the thickness LPG of the membrane bilayer (Kirschner and Blaurock, 1992). For an overview of the X-ray diffraction experiment used here, the information it provides about myelin

structure, and how this data is related to myelin's electron micrographic image and its lipid bilayer localization, we refer the reader to Fig. 1 in Avila et al. (2005).

The statistical significance for comparisons among the data was evaluated using the Student t-test, with $p < 0.05$ considered as significant. Linear- and pair-correlations, and trendlines were determined using Excel.

3. Results & analysis

3.1. Myelin diffraction was stronger from sciatic nerves than from optic nerves

To quantitate the gradual accumulation of internodal myelin with murine development, we analyzed the X-ray diffraction patterns recorded from intact, mouse sciatic and optic nerves from the postnatal period (4 days for PNS and 15 days for CNS) to about 1.5 years of age. From the youngest to the oldest, the myelin diffraction patterns for both PNS and CNS samples showed a progressive increase in the intensity of the peaks above background, which is the X-ray scatter originating from internodal myelin (Fig. 1). The small shift in position of the intensity maxima suggested an age-dependent change in myelin period (see below).

3.2. Relative amount of internodal myelin increased with age

Plotting $M/(M + B)$ vs. age provided a way to track the relative amount of myelin during development (Fig. 2). This parameter—which reflects the fraction of compact myelin in the nerve volume subtended by the X-ray beam—increased conspicuously with age, particularly at the earliest time points, for both PNS and CNS tissues. The overall greater values for PNS showed there was more myelin in the PNS tissue, and the steeper initial slope in the PNS curve showed that its rate of myelin accumulation was greater than in the CNS (Fig. 2, inset).

As illustrated by the trendlines, three distinct rates of myelin accretion were apparent from the data (Fig. 2). For PNS myelin, the most rapid rate of increase (0.0122 units/day) occurred between days 4 and 20 ($n = 12$). This was followed by a profoundly reduced rate of increase (0.0005 units/day) between days 30 and 180 ($n = 24$), after which there was virtually no change (day 180–495;
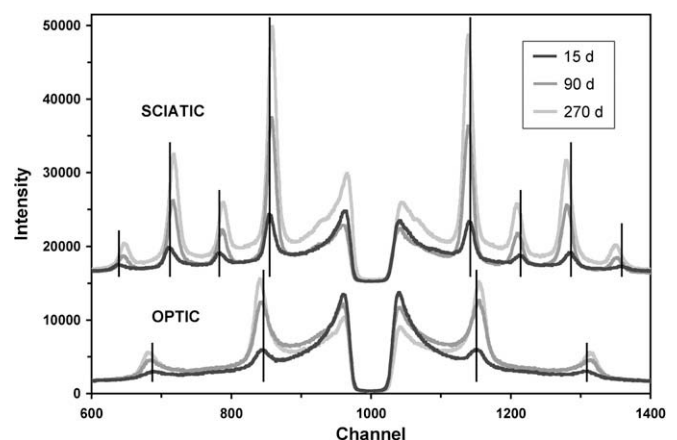
Fig. 1. Diffraction patterns from PNS (sciatic nerve) and CNS (optic nerve) myelin. The progressively stronger peak intensities relative to the total X-ray scatter indicate the accretion of multilamellar internodal myelin. The vertical lines at the peaks indicate the positions of the reflection at the youngest age. In PNS, the shift of peaks toward the center of the pattern with age indicates an increase in period, whereas in CNS the peaks shifted outwards indicating a decrease in period. For clarity, the sciatic nerve patterns have been shifted vertically relative to those from optic nerves.